DE GRUYTER OPEN

ARCHIVES OF MECHANICAL TECHNOLOGY AND MATERIALS
WWW.AMTM.PUT.POZNAN.PL


# Comparison of various tool wear prediction methods during end milling of metal matrix composite

**Martyna Wiciak [a]*, Paweł Twardowski [a], Szymon Wojciechowski [a]**

[a] *Poznan University of Technology, Piotrowo 3 Street, 60-965 Poznan, Poland*

[*] *Corresponding author, Tel.: 790-412-919, e-mail address: martyna.wiciak@put.poznan.pl*

**ARTICLE INFO**

Received 20 October 2017
Received in revised form 23 January 2018
Accepted 29 January 2018

**KEY WORDS**

Tool wear,
Diagnosis,
Milling,
Metal Matrix Composite

**ABSTRACT**

In this paper, the problem of tool wear prediction during milling of hard-to-cut metal matrix composite Duralcan™ was presented. The conducted research involved the measurements of acceleration of vibrations during milling with constant cutting conditions, and evaluation of the flank wear. Subsequently, the analysis of vibrations in time and frequency domain, as well as the correlation of the obtained measures with the tool wear values were conducted. The validation of tool wear diagnosis in relation to selected diagnostic measures was carried out with the use of one variable and two variables regression models, as well as with the application of artificial neural networks (ANN). The comparative analysis of the obtained results enabled the selection of the most effective tool wear prediction method.

## 1. INTRODUCTION

### *1.1. Characteristics of metal matrix composites MMCs*

Metal matrix composites (MMCs) with their unique physical, mechanical and chemical properties are being widely applied in aerospace and automotive industries. Metal Matrix Composites are materials which consist of alloy metals' matrix reinforced with ceramic particles, i.e. SiC or $Al_20_3$ [5]. Because of high mechanical properties, MMCs are classified as difficult-to-cut. The reinforcement in a form of ceramic particles increases strength, hardness and abrasive wear resistance, which consequently gives an advantage in relation to non-reinforced aluminum alloys [2,3,6].

The unique properties of MMCs allow the competitiveness with heat-resistant super alloys. The reinforcing of material with ceramic particles enables the obtainment of improved ductility, comparing to fiber reinforced metal composites [3].

The most popular MMCs are aluminum alloys reinforced with ceramic particles, e.g. Duralcan™, which is the composite based on aluminum cast alloys reinforced with silicon carbide [1]. This material has found its application in automotive, rail and aerospace industries. The exemplary parts made of Duralcan™ composite include: brake discs, brake calipers, brake pads, brackets, oil sump or elements of steering system. Moreover, the high thermal stability of Duralcan™ castings allows to use as housing of lasers [11].

Machining of MMCs introduces the difficulties because of hard silicon carbide content, which improves the exploitation properties of composite, however from the other side, it simultaneously contribute to the rapid tool wear [2,4]. The ceramic inclusions are harder than tungsten carbide and other materials which are being intended to cutting tools. When the cutting edge during machining is contacted with hard ceramic particles, then micro chipping of the tool can occur [12].

### *1.2. Diagnostics of machining process*

The primary objective of machining technology is the maintaining of high and constant quality together with

DOI: 10.2478/amtm-2018-0001

minimization of costs. One of the factors, which directly affect the machining requirements are machine stoppage times. Thus, their minimization is of high importance [8]. Because of high quality requirements, the cutting tools are very often being changed, which consequently elongates the stoppage times. Therefore, the efficient diagnosis of a machining is essential in order to the process enhancement. In a range of a machining technology, three areas of diagnostics can be distinguished: diagnosis of tool condition, diagnosis of machine's technical condition and diagnosis of workpiece quality. During the diagnosis of machining process, the information about the tool wear or its catastrophic failure is usually important [7].

Diagnosis of machining is mainly focused on the detection of tool wear extent. The application of various phenomena connected with machining allows the diagnosis of cutting tool. It is based on the measurement of signals, which are connected with the tool wear, i.e. the growth of cutting force, acoustic emission (AE), mechanical vibrations, temperature or noise level.

The prediction of tool wear is a complex problem, especially when the cutting conditions are variable. However the growing development of monitoring systems enables the improved assessment.

Currently, the advanced signal processing methods are being applied, which allow the determination of measures connected with many types of signals and simultaneously the selection of measures applicable to diagnostics [7].

In the area of machining process diagnostics, the diagnostic inference methods are based on the pseudo-deterministic model. However, during the tool condition diagnosis, the fundamental methods are based on the regression and pattern recognition approaches [10].

Neural networks, as the one of pattern recognition methods, reach the growing interest because of their elasticity, computational power and simplicity of use. With the use of this modeling technique, the possibility of complex functions' projection can be reached. The primary feature of neural networks is automatic learning on the basis of data introduced by the user. As a consequence, it leads to generation of the searched model by the network itself.

The primary and the most frequently applied neural network is multi-layered perceptron (MLP). Based on neuron's inputs, the mean weighted value is being calculated, with the use of transmittance function and given in a form of a result at the output of the network. Multi-layered perceptron is a simple model with the input and output, and appropriately selected weights [9].

Because of high reliability, the neural networks are being applied to machining process diagnosis, and the most frequently: to tool wear diagnosis. On the basis of many researches one can observe that the most popular network is multi-layered perceptron, which application gives the satisfactory results.

## 2. EXPERIMENTAL DETAILS

### *2.1. Research range*

The objective of research involved the diagnosis of tool condition, based on the measurement of vibrations during end milling of MMC.

The Duralcan™ metal matrix composite has been selected as a workpiece. The reinforcement of aluminum alloy with the hard SiC particles (approx.10 %) allowed the improvement of mechanical properties together with improved abrasion resistance.

Figure 1 depicts the microstructure of the workpiece. The MMC was obtained with the application of die casting.

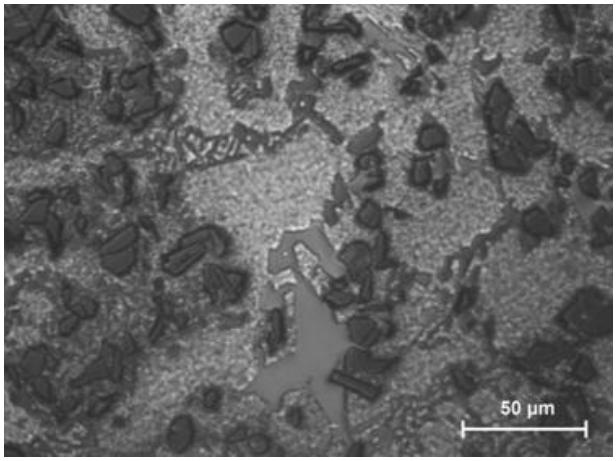


***Fig. 1. The microstructure of MMC***

Table 1 depicts the chemical composition of the workpiece.

The monolithic end mills MaxiMet™ by Kennametal were selected as the cutting tools (Fig. 2). They were made of fine-grained tungsten carbide.

***Tab. 1.The chemical composition ofDuralcan™***

| Element | Si | Fe | Cu | Mg | Ti | Al |
|---|---|---|---|---|---|---|
| [%] | 8,50 – 9,50 | 0,20 max | 0,20 max | 0,45 – 0,65 | 0,20 max | rest |

In order to check the repeatability of the measurements, the six identical 3-toothed mills were applied during the machining tests, conducted in the constant cutting conditions.

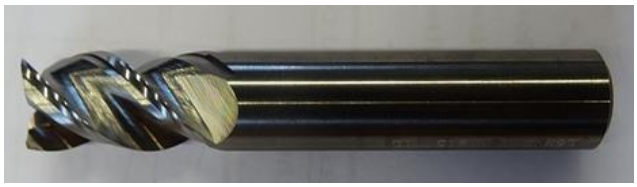

***Fig. 2. Monolithic end mill MaxiMet™ Kennametal***

The milling tests were conducted on AVIA FND-32F milling machine, with the cutting conditions presented in table 2.

***Tab. 2. Cutting conditions***

| | |
|---|---|
| Rotational speed $n$ [rev/min] | 1400 |
| Cutting speed $v_c$ [m/min] | 44 |
| Feed per tooth $f_z$ [mm/tooth] | 0,02 |
| Feed rate $v_f$ [mm/min] | 84 |
| Cutting path $L$ [mm] | 278 |
| Cutting depth $a_p$ [mm] | 5 |
| Cutting width $a_e$ [mm] | 0,5 |

### 2.2. Research method

The measurements of accelerations of vibrations were carried out with the application of three-directional piezoelectric Brüel & Kjær 4321 sensor clamped to the machine's fixture. The measurements were conducted in the following directions: X – feed direction $A_f$, Y – feed normal direction $A_{fN}$ and Z – thrust direction $A_p$.

The amplification and processing of signals acquired by the sensor was carried out with the use of Brüel & Kjær NEXUS 2692-C amplifier. Additionally, the A/D transducer located in a PC was applied. Figure 3 shows the experimental apparatus set-up.

The analysis of the obtained signals was conducted with the application of the dedicated software. This program allowed the generation of vibration signals in time and frequency domain. The analysis involved the use of the following statistical measures: root mean square value $A_{i\_RMS}$ and peak value $A_{i\_peak}$.

After the measurement of vibrations during the one milling pass, the tool flank wear $VB_B$ on the tool's rectilinear section was inspected with the use of microscope. The tool flank wear $VB_B$ was measured for three cutting edges of each tool. The value of the tool flank wear was averaged. The dullness criterion for the milling tool was equaled to $VB_{B\_gr}$ = 0,3 mm.

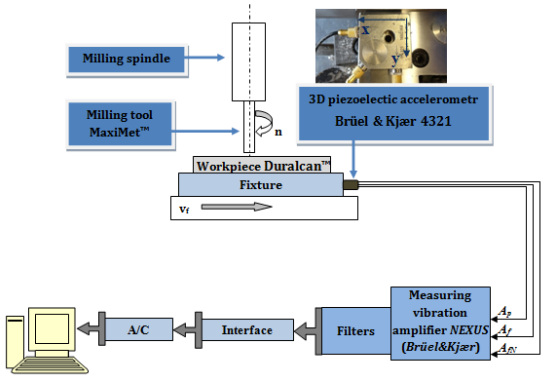


*Fig. 3. The set-up of experimental apparatus*

## 3. RESULTS AND DISCUSSION

### 3.1. Analysis of tool wear

Research results show the measured tool flank wear and the acceleration of vibrations generated during end milling of MMC.

Figure 4 depicts tool flank wear $VB_B$ values in function of time for the all investigated end mills.

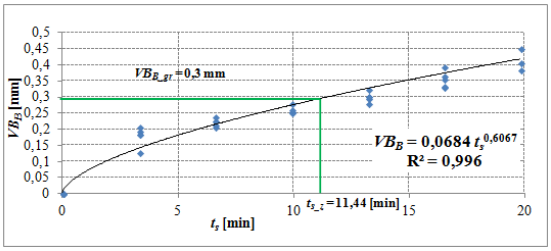


*Fig. 4. Tool flank wear in function of time for the investigated end mills*

In order to determine the relations between the tool wear $VB_B$ and cutting time, the power function has been selected: $VB_B = a \cdot t_s^n$. On the basis of the determined equation, the average time needed for the excessing the critical tool wear value has been calculated as: $t_{s\_z}$ = 11,44 min.

The cutting tools which are recommended to machining of Duralcan™ composite are polycrystalline diamonds PCD, because of relatively high tool life, correlated with higher hardness of PCD in comparison to SiC reinforcing phase of MMC. Nevertheless in this work, the end mills made of tungsten carbide were applied, which are the typical and cheaper equivalent of PCD tools. The analysis of tool wear during the tests confirms that the tool life is significantly shorter than that reached for the PCD tools. The information provided by the Duralcan™ manufacturer reveals that the tool life obtained for the PCD tools is $T \approx 60$ min, when the $VB_{B\_gr}$ = 0,3 mm. In case of tools made of tungsten carbide, the tool life reached for the same dullness criterion is $T$= 11,44 min and thus insufficient. However the conducted research was primarily focused on the evaluation of tool condition diagnosis, as well as the effectiveness of tool wear prognosis.

### 3.2. Analysis of vibrations in time domain

The measured vibrations signals were processed in „*Analizator*" software. The application of this program enabled the generation of vibrations time courses and subsequently the calculation of statistical measures.

After the conducted tests, the tool wear values obtained after the each milling pass were correlated with measured accelerations of vibrations in the three directions. The designations of the selected statistical measures are as follows:

- $A_{f\_RMS}$, $A_{f\_peak}$ – root mean square and peak value of accelerations of vibrations measured in the feed direction (along the X axis),
- $A_{fN\_RMS}$, $A_{fN\_peak}$ - root mean square and peak value of accelerations of vibrations measured in the feed normal direction (along the Y axis),
- $A_{p\_RMS}$, $A_{p\_peak}$- root mean square and peak value of accelerations of vibrations measured in the thrust direction (along the Z axis),

Figure 5 shows the exemplary vibration chart in time domain.

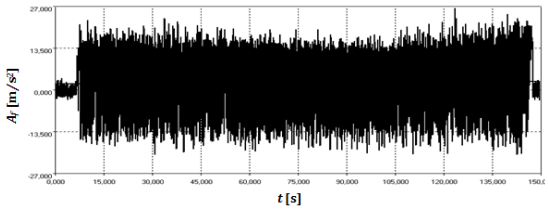


*Fig.5. Vibration time course*

The analysis of vibration charts in time domain can be based on the comparison of amplitudes reached during milling with the new and worn tool. Typically, the growth of tool flank wear leads to the increase of vibration amplitudes. The inference based on vibration amplitude is not usually being applied, because of strong influence of other cutting conditions on the acquired vibration signals, e.g. the effect of cutting speed or spindle's rotational speed, as well as the variations of machining system's dynamical properties.

However, in case of constant cutting conditions, the evaluation of vibration amplitudes can be used as a tool wear symptom.

On the basis of the obtained results, the relation between the tool wear $VB_B$ and specified vibration measure was determined. In order to present the results, the whole experimental series was taken into account.

Figure 6 shows the exemplary chart containing the linear equation between the tool wear and vibrations:$VB_B = a \cdot A_{i\_RMS(peak)} + b$. The conformity of the experimental results with the selected function can be described by the $R^2$ coefficient.

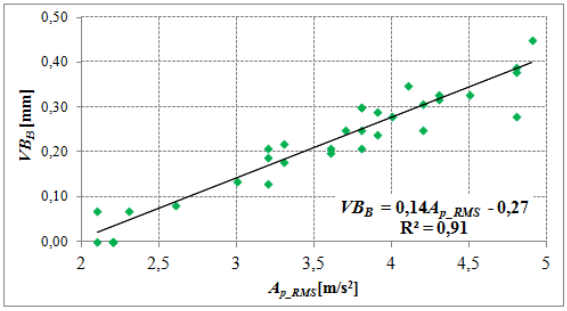


***Fig. 6. Relation between $VB_B$ and $A_{p\_RMS}$***

### *3.3. Analysis of vibrations in frequency domain*

The subsequent symptom for evaluating the tool wear extent is vibration frequency spectrum. The application of *„Analizator"* software allowed the formulation of vibrations in frequency domain.

On the basis of the generated charts, the tooth passing and tool revolution frequencies, as well as their harmonics were identified.

Figure 7shows the exemplary vibration frequency spectrum generated in *„Analizator"* software.

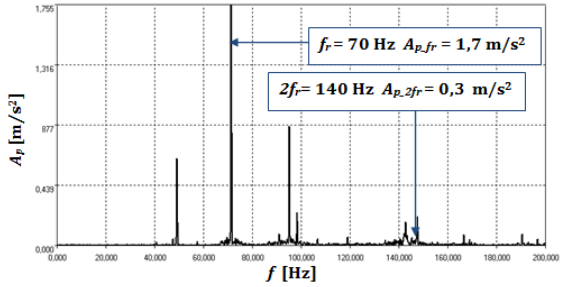


***Fig. 7. The frequency spectrum for the vibrations in the thrust direction***

On the basis of the obtained results, the relations between the tool wear $VB_B$ and constituent corresponding to tooth passing frequency were obtained.

Figure 8 shows the exemplary chart containing the linear function:$VB_B = a \cdot A_{i\_fr(2fr)} + b$.

Formulation of diagnostic model allows the prognosis of tool wear values. The first developed diagnostic model was one based on one variable regression function. It is the open mathematical function, which determines the relations between the $VB_B$ tool wear indicator and specified measure of diagnostic signal.

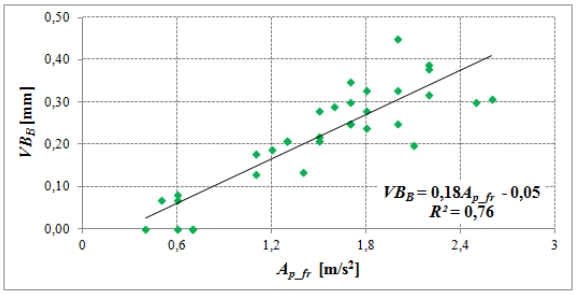


***Fig. 8. Relation between $VB_B$ and $A_{p\_fr}$***

### *3.4. Diagnostic inference based on one variable regression model*

The obtained function allows the determination of tool wear $VB_B$ expected value based on value of the diagnostic measure.

The one variable regression model was described by the following mathematical function:$VB_B = a \cdot A_i + b$. Tables 3 and 4 summarize the determined functions with $R^2$ Coefficient.

***Tab. 3. One variable regression model for the measures determined in time domain***

| Function | Coefficient $R^2$ |
|---|---|
| $VB_B = 0{,}03A_{f\_RMS} + 0{,}02$ | $R^2 = 0{,}11$ |
| $VB_B = 0{,}02A_{f\_peak} - 0{,}16$ | $R^2 = 0{,}38$ |
| $VB_B = 0{,}01A_{fN\_RMS} + 0{,}11$ | $R^2 = 0{,}05$ |
| $VB_B = 0{,}01A_{fN\_peak} - 0{,}06$ | $R^2 = 0{,}26$ |
| $VB_B = 0{,}14A_{p\_RMS} - 0{,}27$ | $\mathbf{R^2 = 0{,}91}$ |
| $VB_B = 0{,}03A_{p\_peak} - 0{,}20$ | $R^2 = 0{,}62$ |

***Tab. 4. One variable regression model for the measures determined in frequency domain***

| Function | Coefficient $R^2$ |
|---|---|
| $VB_B = 0{,}01A_{f\_fr} + 0{,}17$ | $R^2 = 0{,}06$ |
| $VB_B = 0{,}10A_{f\_2fr} + 0{,}05$ | $R^2 = 0{,}48$ |
| $VB_B = 0{,}01A_{fN\_fr} + 0{,}15$ | $R^2 = 0{,}10$ |
| $VB_B = 0{,}08A_{fN\_2fr} + 0{,}08$ | $R^2 = 0{,}40$ |
| $VB_B = 0{,}18A_{p\_fr} - 0{,}05$ | $\mathbf{R^2 = 0{,}76}$ |
| $VB_B = 0{,}24A_{p\_2fr} + 0{,}13$ | $R^2 = 0{,}12$ |

The $R^2$ coefficient has been applied for the searching of the best diagnostic measure. The selection of the best measure is determined by the $R^2$ value which should be as close as possible to 1. Tables 3 and 4 reveal that the most appropriate measures for the tool wear diagnosis are $A_{p\_RMS}$ and $A_{p\_fr}$. The both measures are based on the vibration thrust direction.

In order to validate the one variable regression model, the one of the end mills has been selected as the verifying tool. The values of the particular measures for the fifth end mill were not taken into account intentionally during the formulation of $VB_B = a \cdot A_i + b$mathematical function. This approach aimed at validation of tool wear prognosis, based on completely new values, which have not been previously

considered as the input data during the formulation of function.

In order to validate, the two best measures from the time and frequency domain were selected:

$A_{p\_RMS}$ ($R^2$ = 0,91), $A_{p\_peak}$ ($R^2$ = 0,62) and $A_{p\_fr}$ ($R^2$ = 0,76), $A_{f\_2fr}$ ($R^2$ = 0,48).

Figure 9 shows the exemplary chart describing the dependencies between the value of tool wear $VB_{B\_rz}$ measured during the milling tests with the verifying tool and the value determined on the basis of regression function for the specified diagnostic measure. In order to evaluate the error value, the $e$ parameter, describing the conformity has been introduced. The mean square error was calculated on the basis of equation:

$$e = \sum_{i=1}^{N}(VB_{B\_tei} - VB_{B\_rzi})^2 \quad (1)$$

where:
$N$ – number of data points,
$VB_{B\_tei}$ – predicted value,
$VB_{B\_rzi}$– real value.

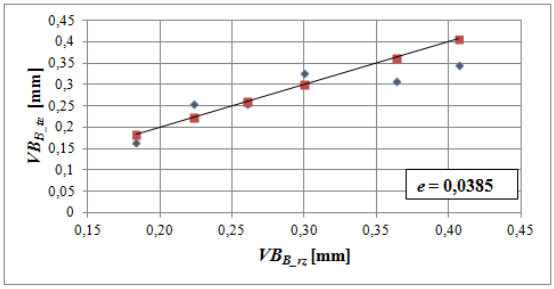


***Fig. 9. Relation between the real and predicted tool wear values for the $A_{p\_fr}$ measure $VB_B = 0{,}18A_{p\_fr} - 0{,}05$***

On the basis of the Fig. 9 one can evaluate the efficiency of the specified diagnostic model. The best fitted model can be described by the function: $VB_B = 0{,}18A_{p\_fr} - 0{,}05$. The calculated error between the real and predicted value is in this case the smallest ($e$ = 0,0385). Based on the obtained results, one can note that not any of the measures can be applied to the tool wear prognosis, because the predicted values significantly differ from the expected value.

The obtained error is acceptable and can be indicative of a good quality of the determined regression function.

### 3.5. Diagnostic inference based on two variables regression model

The next diagnostic inference method during the research was multivariate regression model. During this approach the tool wear value is being determined with the use of a many measures (from one or more signals). In order to formulate the model, the *„Statistica"* software has been applied. The regression function in the form of second order polynomial was used. The selection of the two best measures was based on the evaluation of $R^2$ coefficient, similarly to the approach with the one variable regression model.

Table 5 depicts various configurations of measures and second order polynomial equations for the each model.

The exemplary two variables regression model, generated in *„Statistica"* software is presented in Figure 10.

Subsequently, the dependency between the value of tool wear $VB_{B\_rz}$ measured during the milling tests with the verifying tool and the value determined on the basis of the two variable regression function was determined. The $e$ parameter has been selected once again as an error function.

Figure 11 shows the level of conformity between the real and the predicted values. The fifth milling tool has been selected as a verifying tool.On the basis of the determined dependencies one can identify the model which has the highest accuracy of the tool wear prediction. The smallest error was obtained for the one variable regression model developed for the $A_{p\_fr}$ and $A_{p\_peak}$ measures. This model can be stated as the most efficient to tool wear prognosis.

***Tab. 5. Two variables regression functions***

| Selected measures | Function in a form of second order polynomial |
|---|---|
| $A_{p\_fr}$ and $A_{p\_peak}$ **$R^2$ = 0,82** | $VB_B = -0{,}1489 + 0{,}1829 \cdot A_{p_{fr}} + +0{,}0085 \cdot A_{p_{peak}} - 0{,}0922 \cdot A_{p_{fr}}{}^2 + +0{,}0138 \cdot A_{p\_fr} \cdot A_{p\_peak} - 0{,}0006 \cdot A_{p\_peak}{}^2$ |
| $A_{p\_fr}$ and $A_{p\_RMS}$ **$R^2$ = 0,91** | $VB_B = -0{,}3455 - 0{,}1146 \cdot A_{p_{fr}} + +0{,}2346 \cdot A_{p_{RMS}} - 0{,}0534 \cdot A_{p_{fr}}{}^2 + +0{,}0879 \cdot A_{p\_fr} \cdot A_{p\_RMS} - 0{,}035 \cdot A_{p\_RMS}{}^2$ |
| $A_{p\_RMS}$ and $A_{p\_peak}$ **$R^2$ = 0,94** | $VB_B = -0{,}2384 + 0{,}012 \cdot A_{p_{peak}} + +0{,}0683 \cdot A_{p_{RMS}} - 0{,}0028 \cdot A_{p_{peak}}{}^2 + +0{,}0201 \cdot A_{p\_peak} \cdot A_{p\_RMS} - 0{,}0317 \cdot A_{p\_RMS}{}^2$ |
| $A_{p\_RMS}$ and $A_{f\_2fr}$ **$R^2$ = 0,91** | $VB_B = -0{,}3092 + 0{,}1282 \cdot A_{p_{RMS}} + +0{,}0828 \cdot A_{f_{2fr}} + 0{,}009 \cdot A_{p_{RMS}}{}^2 - -0{,}0381 \cdot A_{p\_RMS} \cdot A_{f\_2fr} + 0{,}0166 \cdot A_{f\_2fr}{}^2$ |

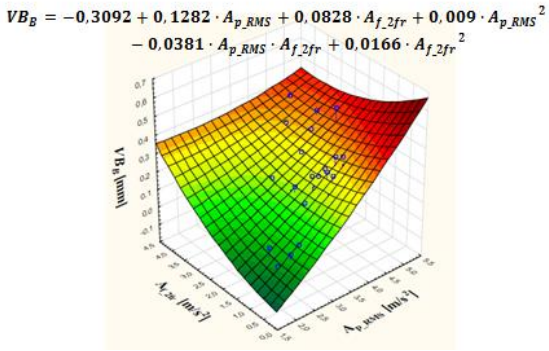


***Fig. 10. Two variables regression model for $A_{p\_RMS}$ and $A_{f\_2fr}$***

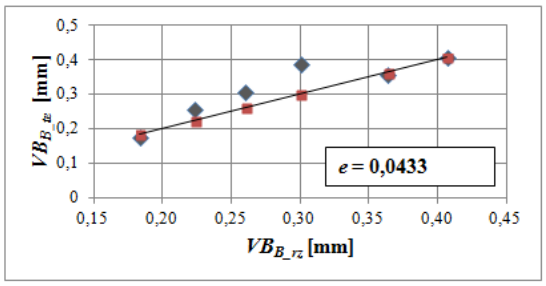


***Fig. 11. Relation between the real and predicted tool wear values ($A_{p\_fr}$, $A_{p\_peak}$)***

### 3.6. Diagnostic inference based on artificial neural networks

One of the most frequently applied inference models are pattern recognition methods. Neural networks are recognized as one of the most efficient tool wear prognosis methods. During this work the *MLP (MultiLayer Perceptron)* was applied. Moreover for the comparison, the *RBF (Radial Basis Function*) was also employed.

The simplest approach to statistical inference is association of input variables $x$ with continuous output variable, which consequently enables the obtainment of information regarding the relations between the data. The various diagnostic measures were introduced as the output variables, whereas the tool wear $VB_B$ was the constant output value.

The ANN diagnostic model was formulated in *„Statistica"* software and *„Neural networks"* module .In order to search the network with the best quality, the various configurations of diagnostic measures with the application of various number of hidden layers were introduced and checked.

The one-directional network's structure is being achieved based on signal's flow from the input neurons, through the hidden ones, and finally to the output neurons. Applying the automatic network's searching, the program itself suggests the best fitted function to the particular case.

Table 6 shows the various configuration of diagnostic measures which were applied as an input data.

***Tab. 6. The overview of input data configurations***

| No. | Number of input data | Input data |
|---|---|---|
| 1. | 6 | $A_{f\_RMS}$, $A_{f\_peak}$, $A_{fN\_RMS}$, $A_{fN\_peak}$, $A_{p\_RMS}$, $A_{p\_peak}$ |
| 2. | 6 | $A_{f\_fr}$, $A_{f\_2fr}$, $A_{fN\_fr}$, $A_{fN\_2fr}$, $A_{p\_fr}$, $A_{p\_2fr}$ |
| 3. | 4 | $A_{p\_RMS}$, $A_{p\_peak}$, $A_{p\_fr}$, $A_{f\_2fr}$ |
| 4. | 3 | $A_{p\_RMS}$, $A_{p\_peak}$, $A_{p\_fr}$ |
| 5. | 3 | $A_{p\_peak}$, $A_{p\_fr}$, $A_{f\_2fr}$ |
| 6. | 2 | $A_{p\_RMS}$, $A_{p\_peak}$ |

After the entering of various input data to the program and the selection of hidden layers' size, the learning process has been conducted. During this process, the best weights' values, which connect the inputs with the hidden neurons, were searched with the application of the iterative approach. According to this algorithm, the weights are being fitted to the neurons in a way enabling the minimization of differences between the network's output and the real value. After the learning process, the comparison of outputs with the learned data is being carried out.

As an objective, the reduction of differences between the network's outputs and entered outputs is being conducted.

Table 7 depicts the examples of applied neural networks.

After the network's learning process, the prediction accuracy for the completely new data was checked. Similarly to one and two variables regression models, the validation data have stated the values of specified diagnostic measures obtained during the milling tests with the fifth end mill.

Based on the validation data, the predicted value of the tool wear was determined. Figure 12 shows the exemplary chart, describing the dependencies between the real value of the tool wear $VB_{B\_rz}$ and theoretical value $VB_{B\_te}$ for the applied model, together with the determined validation error.

On the basis of the validation error, the evaluation of neural network's activity correctness was conducted. It was stated that the validation error is decreasing together with the elimination of particular measures on the network's input. In this case, the application of higher amount of input data is not improving the quality of network's activity. The lowest error was reached when the three following diagnostic measures: $A_{p\_RMS}$, $A_{p\_peak}$, $A_{p\_fr}$ were introduced. The selection of these three measures was not coincidental, because they were identified on the basis of information obtained from the previous analyses. These diagnostic measures reached the highest correlation coefficient $R^2$.

***Tab. 7. Results from the various types of ANNs***

| Type of network | MLP 6-8-1 | RBF 4-7-1 | MLP 3-4-1 |
|---|---|---|---|
| Number of inputs | 6 | 4 | 3 |
| Number of hidden layer's neurons | 8 | 7 | 4 |
| Learning quality | 0,9817 | 0,9591 | 0,9506 |
| Testing quality | 0,9692 | 0,9857 | 0,9974 |
| Learning error | 0,0003 | 0,0007 | 0,0008 |
| Testing error | 0,0012 | 0,0005 | 0,0001 |
| Activation function | Exponential | Linear | Linear |

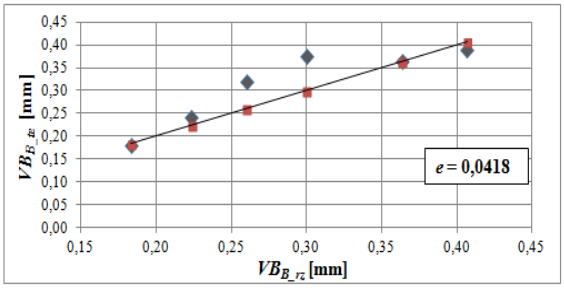


***Fig. 12. Validation of MLP 3-4-1 ($A_{p\_RMS}$, $A_{p\_peak}$, $A_{p\_fr}$)***

The comparison of *MLP* with *RBF* have revealed that there are no significant differences in relation to their quality. The validation errors were similar, however the learning and testing quality was lower in case of *RBF* network.

### 3.7. Comparison of inference methods

The comparative analysis of the results aimed at identification of the most accurate diagnostic model to tool wear prognosis. The evaluation considers three inference methods, namely: the one variable regression model, the two variables regression model and artificial neural network.

In order to compare the efficiency of the applied models, the error $e$ values were summarized.

Table 8 depicts the applied models together with the collection of obtained errors. It should be emphasized that ideal case can be met when the error $e = 0$, then all points will be located on the straight line. Practically, all models are characterized by the occurrence of errors, however the higher discrepancies form the line indicates the worse fitting

of the diagnostic model. Therefore, the searching was focused on the model with the lowest mean square error.

Evaluating the obtained results, one can note that the best results were reached for the single variable regression model. Nevertheless, when the repeatability of the results was taken into account, this model was characterized by the highest discrepancies.

***Tab. 8. Overview of errors e for the compared models***

| One variable regression | Two variables regression | Pattern recognition model | |
|---|---|---|---|
| 0,0823 | **0,0433** | 0,0591 | **0,0418** |
| 0,1533 | 0,0480 | 0,0630 | 0,0507 |
| **0,0385** | 0,0730 | 0,0530 | 0,0535 |
| 0,0824 | 0,0478 | 0,0670 | |

On the basis of the presented results, one can observe that one variable regression model has the highest tool wear value prediction accuracy. Comparing two remaining models, one can observe that error values are comparable, especially in case of ANNs. Despite the fact that these models did not reach the lowest error value, they allow the obtainment of better repeatability and thus they can be also considered in the prediction applications.

Because of computational possibilities of neural networks and capability of learning, these approaches are being frequently applied to tool wear prognosis. The optimization possibilities of entered parameters allows the improvement in network's quality and prediction ability. Considering that tool life is a random variable, even during the application of constant cutting conditions, the ideal fitting of the model is impossible. The application of ANNs is in many cases the best and recommended solution, however in case of MMC milling, the selection of this approach is not optimal.

## 4. CONCLUSIONS

On the basis of the conducted research the following conclusions were formulated.

- The acceleration of vibration signal can be successfully applied for the prediction of tool wear during milling of MMC. However the efficient application of this symptom requires the appropriate processing of signal (i.e. distinguishing the constituents correlated directly with cutting kinematics) and selection of the appropriate vibrations measure.
- The tool wear condition can be described with the highest accuracy when the $A_{p\_peak}$ and $A_{p\_RMS}$ measures are being applied. This was confirmed by the highest value of correlation coefficient. Therefore the vibrations in the thrust direction (along the Z axis) can have the influential effect on the tool wear during milling of MMC.
- The spectral analysis of vibrations reveals also that the correlation coefficient reaches the highest value for the measure regarding the thrust direction: $A_{p\_fr}$. However the conformity is in this case lower for the approx.20% in comparison to that reached for the corresponding measure determined in time domain.
- The application of the two most popular ANNs: *MLP* and *RBF* allowed the identification of the better network. Despite the obtainment of the best learning quality for the network with six input data, the lowest validation error was reached for network with the three inputs. It indicates that for the lower amount of data, the network is able to better fit and evaluate the predicted value.
- Evaluating the results' repeatability, the neural networks and two variables regression model reach better results than the simplest one variable regression model.
- Evaluating the neural networks based on the research, it can be observed that their application is not improving the tool wear prediction accuracy, comparing to other methods. Nevertheless, it is possible that the application of different network types with various number of neurons in a hidden layer could result in a prediction improvement.

## REFERENCES


[1] **Bhattacharya D., Lane C., Lin J.T.,** *Machninability of silicon carbide reinforced aluminium metal matrix composite*, Wear 181-183 (1995) 883-888

[2] **Davim J.,** *Diamond tool performance in machining metal–matrix composites*, Journal of Materials Processing Technology 128 (2002) 100-105

[3] **El-Gallab M., Sklad M.,** *Machning of Al./SiC particulate metal matrix composites Part I: Tool performance*, Journal of Materials Processing Technology 83 (1998) 151-158

[4] **El-Gallab M., Sklad M.,** Machning of Al./SiC particulate metal matrix composites Part II: Workpiece surface integrity, Journal of Materials Processing Technology 83 (1998) 277-285

[5] **Elomari S., Lemieux S.,** *Thermal expansion of isotropic Duralcan metal-matrix composites*, Journal of materials science 33 (1998) 4381-4387

[6] **Frań E., Janas A., A. Kolbus.,** *Porównanie niektórych właściwości mechanicznych kompozytów ex situ typu Duralcan z kompozytami in situ typu Al-TiC*, KOMPOZYTY (COMPOSITES)2(2002)4

[7] **Jemielniak K.,** *Automatyczna diagnostyka ostrzy narzędzi skrawających*, Inżynieria Maszyn, R. 17, z.1, 2012 r.

[8] **Kosmol J.,** *Automatyzacja wytwarzania. Monitorowanie ostrza skrawającego, Metody konwencjonalne i sieci neuronowe*, WNT, Warszawa 1996

[9] **Korbowicz J., Obuchowicz A., Uciński D.,** *Sztuczne sieci neuronowe. Podstawy i zastosowania*, Akademicka Oficyna Wydawnicza PLJ, Warszawa 1994

[10] **Twardowski P.,** *Diagnozowanie i nadzorowanie stanu ostrza i powierzchni obrobionej podczas dokładnego toczenia zahartowanej stali*, praca doktorska, Politechnika Poznańska 1998

[11] www.rtapublicsales.riotinto.com/En/ OurProducts/Documents/FicheDuralcan_Eng-rev%202016-04-19%20CROP.PDF

[12] www.precorp.net/materials/mmc/ (The Duralcan composites machining guidelines)